

RUNNING HEAD: Effect of behavioral state on TMS-evoked response

**Task-Dependent Changes in Cortical Excitability and Effective Connectivity: A
Combined TMS-EEG study**

Jeffrey S. Johnson¹, Bornali Kundu², Adenauer G. Casali³, Bradley R. Postle^{1,4}

1. Department of Psychiatry, University of Wisconsin—Madison, USA
2. Medical Scientist Training Program, University of Wisconsin—Madison, USA
3. Department of Clinical Sciences, Università degli Studi di Milano, Milan, Italy
4. Department of Psychology, University of Wisconsin—Madison, USA

Corresponding Author:

Jeffrey S. Johnson, PhD
Department of Psychiatry
University of Wisconsin-Madison
6001 Research Park Blvd.
Madison, WI 53719

Phone: 1-608-265-8961

Email: jsjohnson3@wisc.edu

Abstract

The brain's electrical response to TMS is known to be influenced by exogenous factors such as the frequency and intensity of stimulation, and the orientation and positioning of the stimulating coil. Less understood, however, is the influence of endogenous neural factors, such as global brain state, on the TMS-evoked response (TMS-ER). In the present study, we explored how changes in behavioral state affect the TMS-ER by perturbing the superior parietal lobule (SPL) with single pulses of TMS and measuring consequent differences in the frequency, strength and spatial spread of TMS-evoked currents during the delay period of a spatial short-term memory task and during a period of passive fixation. Results revealed that task performance increased the overall strength of electrical currents induced by TMS, increased the spatial spread of TMS-evoked activity to distal brain regions, and increased the ability of TMS to reset the phase of ongoing broadband cortical oscillations. By contrast, task performance had little effect on the dominant frequency of the TMS-ER, both locally and at distal brain areas. These findings contribute to a growing body of work using combined TMS and neuroimaging methods to explore task-dependent changes in the functional organization of cortical networks implicated in task performance.

Keywords: EEG, TMS, excitability, effective connectivity, behavioral state

Introduction

Transcranial magnetic stimulation (TMS) is a method that exploits the principle of electromagnetic induction to non-invasively stimulate specific brain areas with the goal of testing hypotheses about brain-behavior relations (Walsh and Pascual-Leone 2003). Although numerous studies have revealed TMS-induced effects on behavioral performance, the endogenous neural factors linking TMS to behavior are at present poorly understood. An important goal of work in this area, therefore, is to uncover the factors that underlie observed variability in the effects of TMS on the brain and behavior. In the present study, we explore the influence of behavioral state on spectral and temporal properties of the TMS-evoked response (TMS-ER).

The brain's response to TMS is known to be influenced by a number of factors specific to particular TMS protocols, including coil orientation (Bonato et al. 2006; Thut et al. 2011) and the intensity and frequency of stimulation (Komssi et al. 2004). Additionally, although the biophysical principles underlying TMS-related current induction are presumably the same for all neural tissue (Walsh and Pascual-Leone 2003), the effect of TMS on brain activity has been found to vary systematically as a function of where on the scalp it is applied. Notably, using combined TMS and electroencephalography (EEG), Rosanova and colleagues (2009) found that single-pulses of TMS elicited a broadband spectral evoked response (ER) that was strongest in the alpha band in occipital cortex (BA 19), in the beta band in parietal cortex (BA 7), and in the high beta/gamma band in frontal cortex (BA 6). They also observed that the characteristic resonant (or "natural") frequency of each

area was preserved across different stimulation intensities, as well as when TMS was applied to distal brain areas. Subsequent experiments have shown that the TMS-ER observed in a given brain area for a particular subject is highly reliable, both within and across sessions, when exogenous parameters of the TMS protocol are held constant (Casarotto et al. 2010). This consistency makes it possible to explore the influence of underlying brain state on the TMS-ER and related behavior.

Previous work has suggested that global brain state also affects the TMS-ER. Examples of this include changes in cortical effective connectivity, relative to the awake state, seen during NREM sleep (Massimini et al. 2005) and following administration of general anesthesia (Ferrarelli et al. 2010). In both cases, the TMS-ER exhibited significantly reduced cortical spread when compared to the ER observed during wakefulness. These findings suggest that variations in the TMS-ER can be used to characterize cortical excitability and changes in the nature of cortical networks that vary with global brain state.

The goal of the present study was to explore how changes in behavioral state influence the TMS-ER. Our approach was to perturb the superior parietal lobule (SPL) with single pulses of TMS, and to compare the evoked response when TMS was delivered during the delay-period of a spatial short-term memory (STM) task versus during passive fixation. Results revealed that task performance increased the overall strength of electrical currents induced by TMS, increased the spatial spread of TMS-evoked activity to distal brain regions, and increased the ability of TMS to reset the phase of ongoing broadband cortical oscillations. By contrast, task

performance had little effect on the dominant frequency of the TMS-ER, either locally or at distal brain areas.

Methods

Subjects

16 subjects participated in this experiment (8 males, mean age = 21.88 [SD=2.94]). All subjects were recruited from the University of Wisconsin-Madison community. The UW-Madison Health Sciences Institutional Review Board approved the study protocols. All subjects gave informed consent and were screened for the presence of neurological and psychiatric conditions and other risk factors related to the application of TMS prior to participation.

Experimental Procedure

To explore task-dependent changes in cortical excitability and connectivity, TMS was delivered during two different behavioral conditions: the delay period of a test of spatial short-term memory (*STM*), and fixation in the absence of a cognitive task (*fixation*). *STM* was operationalized with a spatial delayed-recognition task wherein subjects were instructed to remember the locations of sequentially presented shapes. Each trial began with a 1000-ms fixation period followed by the sequential presentation of four memory targets at different randomly selected locations distributed across each of the four screen quadrants (one shape per quadrant, with quadrant order randomized across trials), as shown in Figure 1. Within each quadrant, memory targets were presented within a $5.5^\circ \times 5.5^\circ$ square region centered $\sim 6.65^\circ$ diagonally from fixation. Memory targets consisted of

abstract shapes (Attneave and Arnoult 1956) subtending $\sim 0.74^\circ$ of visual angle at a viewing distance of 70 cm. Stimuli were black and were presented on a gray background. Each memory target was presented for 200 ms followed by a 400-ms fixation screen. Stimulus presentation was followed by a 3750-ms delay period, during which the central fixation cross remained visible, followed by the appearance of a probe stimulus for 2000 ms. The probe consisted of a black circle ($\sim 0.74^\circ$ of visual angle), and subjects indicated by a yes/no button press whether the location of the probe matched the location of one of the four memory targets (50% probability). For non-match trials, the probe was presented at a different randomly chosen location within one of the four screen quadrants, a minimum of 2.5° (center-to-center distance) away from the memory target location. Subjects were instructed to maintain fixation throughout the delay, and to remember the locations marked by each shape, ignoring shape identity. Feedback was provided on a trial-by-trial basis, with the word "Incorrect" appearing on the screen for 500 ms following an incorrect response. On 50% of trials (randomly interleaved), two TMS pulses were delivered at an average rate of 0.5 Hz during the delay period: The first pulse was delivered 750 ± 250 ms after delay-period onset, followed by the second pulse 2000 ± 250 ms later. Thus, the first TMS pulse could occur as early as 500 ms after the offset of the final memory target, whereas the second pulse could occur as late as 500 ms before the onset of the memory probe. Trials were separated by a 1000-ms ITI. The task block consisted of 160 delayed-recognition trials (80 TMS_{on} and 80 TMS_{off} trials), with a total of 160 TMS pulses delivered during task performance. Subjects were offered a break following every 32 trials (approximately every 5-6 minutes). Prior to

testing, subjects received verbal instructions and completed a block of 16 practice trials (without TMS), which was repeated until a criterion of 75% accuracy was reached (no more than two practice blocks were required for any subject).

In the second type of trial block (block order counterbalanced across subjects), TMS was applied at an average rate of 0.5 Hz during a period of passive fixation. Specifically, TMS was delivered in groups of four pulses while subjects maintained central fixation, with each pulse separated by 2000 ± 250 ms, after which subjects were instructed to “rest and blink” for 2000 ms and the sequence was repeated. A total of 160 TMS pulses were delivered during the fixation block.

TMS targeting and stimulation

TMS was delivered with a Magstim Standard Rapid magnetic stimulator fit with a focal bi-pulse, figure-of-eight 70-mm stimulating coil (Magstim, Whitland, UK). TMS was applied to a portion of the left SPL [Brodmann’s Area (BA) 7] dorsal and medial to the intraparietal sulcus and posterior to the postcentral sulcus (see Figure 1). The SPL was identified on the basis of individual anatomy from whole-brain T1-weighted anatomical MRIs that were acquired with a GE MR750 3T MRI scanner for each subject prior to the experiment (176 axial slices with a resolution of 1mm). TMS targeting was achieved using a Navigated Brain Stimulation (NBS) system (Nextstim, Helsinki, Finland) that uses infrared-based frameless stereotaxy to map the position of the coil and the subject’s head within the reference space of the individual’s high-resolution MRI. The NBS estimates the electrical field induced by TMS on the cortical surface, taking into account the subject’s head shape, the coil position, and scalp-to-cortex distance. TMS stimulation was delivered at an

estimated intensity of 110-140 V/m (65-90% of stimulator output). For each subject, the coil was oriented such that the handle pointed along the sagittal plane (downward), with some adjustments in exact positioning to minimize electrical artifacts at nearby electrodes. With this coil orientation, the direction of induced current was in the anterior-posterior direction perpendicular to the targeted gyrus for the majority of subjects. In several subjects (6 of 16), however, the coil was positioned at a bend in the gyrus, where the orientation of the main axis of the gyrus shifted from perpendicular-to to parallel-to the sagittal plane. In these cases, coil orientation remained approximately parallel to the sagittal plane (i.e., perpendicular to the left-right axis and parallel to the anterior-posterior axis of the targeted gyrus). Importantly, stimulator intensity, and coil position and orientation for a given subject was held constant across the *STM* and *fixation* blocks. Finally, to avoid contamination of the EEG by auditory artifacts, the subject's perception of the clicks produced by the TMS coil's discharge was eliminated by playing masking noise through inserted earplugs throughout the testing session. The volume of the masking noise, which never exceeded 90 dBs, was adjusted immediately prior to the experimental session for each subject until they could no longer hear the TMS discharge.

EEG recording

EEG was recorded with a 60-channel TMS-compatible amplifier (Nexstim; Helenski, Finland). This amplifier avoids saturation by the TMS pulse using a sample-and-hold circuit that holds amplifier output constant from 100 μ s pre- to 2 ms post-stimulus (Virtanen et al. 1999). To reduce additional residual TMS artifacts,

the impedance at each electrode was kept below $3k\Omega$. A single electrode placed on the forehead was used as the reference and eye movements were recorded with two additional electrodes placed near the eyes. Data were acquired at a rate of 1450 Hz with 16-bit resolution.

Data pre-processing

Data were processed offline using the EEGLab toolbox (version 6.01b, Delorme & Makeig, 2004) running in Matlab R2007b (Mathworks, Natick, MA, USA). To begin, the data were down-sampled to 500 Hz and band-pass filtered between 2-80 Hz. A notch filter with a stop band centered at 60 Hz was then applied to reduce line noise evident in the raw EEG. Next, large movement-related artifacts were identified and removed by visual inspection and individual electrodes exhibiting excessive noise were reinterpolated using spherical spline interpolation (Perrin et al. 1989). Independent components analysis (ICA) was then used to identify and remove components reflecting residual muscle activity, eye movements, blink-related activity, and residual TMS-related artifacts (Jung et al. 2000). In general, very few large TMS artifacts were evident in the raw data (mean electrodes exhibiting an artifact = $2.03[\text{min} = 0; \text{max} = 5]$), and what artifacts were present were effectively removed using ICA with little distortion of the EEG waveform. Finally, the data were re-referenced to the average of all 60 electrodes.

Statistical analysis

To explore how task-related changes in brain state influenced the brain's electrical response to TMS, we assessed differences in the amplitude and spectral

power of the TMS-ER under different behavioral conditions (STM versus passive fixation) using cluster-based permutation tests (Maris and Oostenveld 2007) as implemented in the Fieldtrip toolbox for M/EEG analysis (freely available at: <http://fieldtrip.fcdonders.nl/>; Oostenveld et al. 2011). This nonparametric statistical procedure can evaluate conditional data in any combination of time, frequency, and space while controlling for multiple comparisons. The test identifies significant clusters by temporal, spectral, and spatial adjacency, and the quantification of clusters is determined through use of a standard t or F statistic. Any statistic can be used, as the validity and false alarm rate of the test is based on a Monte-Carlo permutation test to determine significant clusters.

Time-domain analysis in sensor space. To assess the main effect of behavioral state on the amplitude and time course of the TMS-ER, we performed a cluster analysis comparing the TMS-ER in the *STM* and *fixation* conditions. For this and all subsequent time-domain analyses, clusters were defined as two or more contiguous sensors in which the t - or F -statistic of amplitude values within individual 2-ms time bins, extending from 0-400 ms post-TMS, exceeded a threshold of $p < 0.05$ ($p < 0.025$ for two-tailed t -tests). Sensors and time points exhibiting above-threshold differences were then used for the subsequent nonparametric cluster-based permutation analysis, which included 500 random sets of permutations. A significance value of .05 was used to threshold the cluster statistic for all analyses.

Frequency-domain analysis in sensor space. To assess the influence of behavioral state on spectral properties of the TMS-ER, the spectral transform of the data was calculated using the Fieldtrip toolbox (Oostenveld et al. 2011). To achieve

sufficient frequency resolution, oscillatory power from 750 ms before to 1250 ms after TMS onset for each condition was estimated using a method in which a frequency-dependent sliding time-window was applied. The window length was 3 cycles/frequency of interest (2-50 Hz, in 1 Hz steps), applied in time-steps of 50 ms throughout the entire 2000-ms trial. The data from each 50-ms time window were then multiplied by a Hanning taper, Fourier transformed, and the power spectral densities were averaged over trials. Spectral estimates for each frequency were baseline corrected on a trial-by-trial basis by subtracting the mean spectral power from the 500 ms window preceding TMS onset for that subject. We used a 500-ms time window (rather than the full 750 ms) to avoid contamination of the baseline period by EEG components related to the processing of the final memory target. The spectral transform of the data was then submitted to the same cluster-based permutation analysis used for the time domain EEG analysis described above. To explore possible longer lasting effects on TMS-evoked oscillations, frequency domain analyses focused on the time window from 0-500 ms post-TMS, which was 100-ms longer than was used for the time-domain analyses. We limited the time window to 500 ms to avoid contamination of time-frequency estimates by transients related to the onset of the memory probe, which could appear as early as 500 ms following the second TMS pulse.

To explore possible changes in the frequency tuning of the SPL under different behavioral conditions, we used the methods of Rosanova et al. (2009) for calculating a region's natural frequency. Specifically, for each condition, the time-frequency matrices were averaged across all channels to obtain a global time-

frequency representation. This allowed us to examine the global brain response to TMS as a function of brain state. The natural frequency of the brain's response in each condition was then determined by averaging the global time-frequency representation over the first 20-200 ms post-TMS and finding the frequency with maximum power. We then conducted a paired *t*-test to determine whether the frequency of the observed spectral response differed between conditions (*STM*, *fixation*).

Frequency domain analysis in source space. To further explore the cortical origins of TMS-evoked responses in the *STM* and *fixation* conditions, we conducted a parallel analysis in source space. The source solution would theoretically decrease conduction effects and provide a more accurate power distribution from the estimated neural sources of oscillation generators. Source modeling was performed using the methods described in Casali et al. (2010), wherein individual cortical meshes (3004 or 5124 vertices)¹ were created using the Statistical Parametric Mapping software package (SPM5 and SPM8, freely available at: <http://www.fil.ion.ucl.ac.uk/spm>). This involved warping the binary masks of the skull and scalp obtained from individual MRIs to the corresponding meshes of the Montreal Neurological Institute (MNI) atlas. Additionally, skull and scalp meshes were created and co-registered with EEG sensors by rigid rotations and translations of digitized landmarks (nasion, left and right tragus). Next, a 3-spheres BERG method (Berg and Scherg 1994) was used to model conductive head volume and

¹ For a subset of subjects, suitable cortical meshes could not be created using SPM5. For these subjects, SPM8 was used. Differences in the number of vertices reflect the minimum number of vertices available in SPM5 and SPM8, respectively.

calculate the Lead Field Matrix using the Brainstorm software package (freely available at: <http://neuroimage.usc.edu/brainstorm>). The inverse solution was then calculated on a trial-by-trial basis using an empirical Bayesian approach as implemented in SPM5 (Friston et al. 2002; Phillips et al. 2005; Tikhonov and Arsenin 1977). For this analysis, the covariance matrix was assumed independent across EEG electrodes, and covariance components were modeled by two priors: the Weighted Minimum Norm (WMN) constraint and a Gaussian distribution of source covariance along the geodesic (smoothness parameter = 8 mm), which enforced correlation among neighboring sources. These priors were estimated directly from the data using restricted maximum likelihood (Friston et al. 2006; Friston et al. 2002; Mattout et al. 2006; Phillips et al. 2005). Finally, to compute the overall current evoked by TMS in different cortical areas, individual cortical surfaces were attributed to different Brodmann areas using an automatic anatomical classification method that maps the individual cortical surface to the ROI (region-of-interest) masks provided by the WFUPickAtlas tool (freely available at: <http://ansir.wfubmc.edu>; Maldjian et al. 2003).

To analyze spectral properties of the TMS-ER in source space, we calculated the event-related spectral perturbation (ERSP) from 750 ms before to 1250 ms after TMS onset for each condition. ERSPs were computed using a moving Hanning-windowed wavelet with 3 cycles for the lowest frequency (4 Hz) increasing linearly to 18 cycles for the highest frequency analyzed (50 Hz). Responses were baseline corrected for each subject by subtracting the calculated mean ERSP from the 500 ms window preceding TMS onset for that subject.

Excitability and effective connectivity analysis in source space. Because of the causal nature of the TMS-ER, the pairing of TMS with EEG can also be used to measure effective connectivity. That is, whereas functional connectivity is inferred from patterns of covariation between anatomically distinct regions A and B, when TMS is delivered to A the TMS-ER at B gives a causal (rather than correlative) indication of the coupling between the two. To quantitatively evaluate behavioral-state related differences in cortical excitability and effective connectivity, the source-localized data were submitted to a standardized, data-driven procedure that characterizes the electrical response of the brain to TMS by means of three synthetic indices (Casali et al. 2010): significant current density (SCD), phase-locking (PL), and significant current scattering (SCS). SCD is expressed in units of $\mu\text{A}/\text{mm}^2$ and represents the sum of the absolute amplitude of all significant TMS-evoked currents observed over a given time interval and/or cortical region, which were identified using a non-parametric statistical procedure. PL reflects the ability of TMS to reset the phase of ongoing oscillations and can be computed as either a broad-band (bPL) or a narrow-band (nPL) index focusing on different components of the EEG spectrum. PL is dimensionless and ranges from 0 (random phases) to 1 (perfect phase locking), and is orthogonal to the amplitude of ongoing oscillations, emphasizing the temporal coherence of oscillations over time and space. Finally, SCS is calculated as the sum of the geodesic distances (in mm) between the stimulated brain region and any significant current source over a given time interval and cortical volume. Thus, this index captures the spatial spread of TMS-evoked currents to distal brain regions, growing proportionally larger as significant TMS activations

spread away from the targeted brain area. Taken together, these synthetic indices can be used to characterize different properties of the stimulated cortical area, from its local excitability to its connectivity with other brain regions, and how these properties may change under different conditions.

Results

Behavioral data

Performance of the STM task was largely unaffected by concurrent delay-period TMS, with mean accuracy (% correct) of 84.06 (SD=8.75) and 84.38 (SD=8.37), and mean reaction time (RT) of 735.90 (SD=121) and 722.66 (SD=128.09) ms in the TMS_{off} versus TMS_{on} conditions, respectively. Confirming this, separate one-way repeated-measures ANOVAs with TMS (On, Off) as a within-subjects factor revealed no significant effects of TMS on either accuracy or RT (all $ps > .09$).

EEG data

The effect of behavioral state on the amplitude of the TMS-ER. Figure 2a-b shows the average TMS-ER recorded over two separate clusters of electrodes (see inset topographical plots) in the *STM* and *fixation* conditions. As can be seen in each plot, the overall shape and amplitude of the waveform is remarkably similar across behavioral conditions, particularly in the first 75 ms post-TMS. After this time, the waveforms begin to diverge to some extent, with a larger negative deflection at midline electrode sites (Fig. 2b) in the *STM* versus *fixation* condition beginning around 70 ms post-TMS. Coincident with this, a strong positive deflection was observed in the *STM* condition over more lateral electrode sites (Fig. 2a) in the same

time window. The amplitude of the TMS-ER was also somewhat larger in the *STM* versus *fixation* conditions over central midline electrode sites beginning around 200 ms, shifting to more lateral and posterior electrodes from 260-280 ms (Fig. 2b). In keeping with these observations, cluster analysis (Fig. 2c) revealed a significant negative cluster ($STM < fixation$) of central midline electrodes beginning ~60-80 ms post-TMS, and a significant positive cluster ($STM > fixation$) of more peripheral electrodes (all $ps < 0.05$) beginning ~100 ms post-TMS. Additionally, a second positive cluster was observed over central midline electrodes from 200-260 ms, shifting to more lateral and posterior electrodes from 260-300 ms post-TMS. Taken together, these clusters appear to reflect an overall increase in amplitude of a lower-frequency component of the TMS-ER in the *STM* condition, beginning around 60 ms and extending to ~300 ms post-TMS. This outcome anticipates the results of the effective connectivity analyses, which are presented further along in this section.

The effect of behavioral state on spectral properties of the TMS-ER. Our first frequency-domain analysis focused on determining the natural frequency of TMS-evoked oscillations, and whether this changed as a function of behavioral state. Using the methods of Rosanova et al. (2009), in which a single frequency exhibiting maximum power during the first 200 ms following TMS is identified, we estimated the natural frequency of the SPL to be in the lower beta band with mean frequency 16.75 Hz (SD=12.41 Hz) in the *fixation* condition and 13.69 Hz (SD=10.34 Hz) in the *STM* condition, a difference that was not statistically reliable, $t(11) = 0.87$, n.s. However, as can be seen in the aggregate data depicted in Figure 3, in many cases the frequency spectrogram took on a bimodal distribution consisting of a short-

duration, relatively high-frequency peak together with a longer-lasting, lower-frequency peak. The high-frequency component of the TMS-ER was centered at 19 Hz in both the *STM* and *fixation* conditions. The second peak was slightly lower frequency in the *STM* versus *fixation* condition (6 Hz vs. 8 Hz, respectively), and appeared to be higher amplitude and of longer duration.

To explore this more fully, our second analysis focused on the effects of behavioral state on the power of TMS-evoked oscillations. Recall that, for the corresponding analysis in the time domain, we found significant clusters beginning at approximately 60 ms and extending to 300 ms post-TMS (Fig. 2). This seemed to reflect an overall larger amplitude low-frequency component of the TMS-ER in the *STM* versus *fixation* condition. Although, as noted above, there does appear to be a larger sustained low-frequency oscillation in the *STM* condition in the analysis of the spectrally transformed data throughout the post-TMS interval (see Fig. 3a), the only significant cluster found was in the beta and gamma bands from ~200-400 ms, for which broadband high-frequency power was greater in the *STM* condition (see red dashed boxes in both panels of Fig. 3).

The effect of behavioral state on the natural frequency of the TMS-ER at local and distal cortical sources. Figure 4 shows the time-frequency decomposition of TMS-evoked oscillations at the local source level from four cortical areas of interest (BA 6, BA 7, BA 8, and BA 19) in the *STM* (Fig. 4a) and *fixation* (Fig. 4b) conditions following TMS of the SPL (BA 7). Figure 4c shows the mean TMS-evoked power from 4-50 Hz averaged across the first 200 ms following TMS for both behavioral conditions. As can be seen, TMS of BA7 during the *fixation* condition produced a

dominant frequency of 9 Hz in BA 19, 24 Hz in BA 7, and 27 Hz in BA 6. Very similar values were observed in the *STM* condition (BA 19 = 8 Hz, BA 7 = 22 Hz, BA 6 = 30 Hz).

Because the superior frontal cortex, including the territory of the frontal eye fields (FEF), has also been found to be engaged during the performance of spatial memory tasks (e.g., Courtney et al. 1998; Curtis and D'Esposito 2003; Postle et al. 2000), we were also interested in whether TMS-evoked activity would be higher in this area when TMS was applied during the delay period of the *STM* task. In keeping with this possibility, a prominent, sustained low-frequency oscillation was observed in BA 8 in the *STM* condition ($M = 6$ Hz, see Fig. 4, rightmost column), which was much larger than a similar sustained oscillation observed in the *fixation* condition ($M = 5$ Hz). A similar low-frequency oscillation is also evident in the time-frequency plot of TMS-evoked activity in BA 6, where the posterior portion of the FEF is found in humans (Curtis and D'Esposito 2003), which was particularly pronounced during task performance. This may reflect the source of the prominent low-frequency component of the TMS-ER observed from ~75-300 ms at the scalp level (see Fig. 2a-c).

The effect of behavioral state on the strength and spatial spread of TMS-evoked currents. Our analysis of behavioral state-related differences in the TMS-ER at the scalp level suggested that the TMS-ER may be larger in amplitude, both locally and at distant cortical sites, when TMS is applied during the performance of a task. Thus, to explore possible task-related differences in cortical excitability and effective connectivity, we used the methods of Casali et al. (2010) to derive a set of synthetic

measures for characterizing the brain's electrical response to TMS from the source-localized data. Figure 5a-b shows results from the *STM* and *fixation* conditions for each index, averaged over subjects. As can be seen, the overall strength of electrical currents induced by TMS (Significant Current Density, SCD), the overall spatial spread of TMS (Significant Current Spread, SCS), and the ability of TMS to reset the phase of ongoing oscillations (broadband Phase Locking, bPL) were all greater when TMS was applied during the delay interval of the *STM* task. This was confirmed in a series of one-tailed t-tests comparing SCD, SCS, and bPL in the *STM* versus *fixation* condition (all $t_s > 2.18$).

Figure 5c shows the average spatial distribution of SCD, SCS, and bPL across subjects in each behavioral condition. As can be seen, TMS induced significant currents and reset the phase of broadband oscillations at the stimulated area (green arrows) and in bilateral parietal and frontal areas, as well as, to a lesser degree, in inferior parietal and occipital cortical areas. The spread of TMS-evoked currents to distal brain areas as well as the ability of TMS to reset the phase of ongoing oscillations was particularly pronounced in the *STM* condition. This suggests that task performance increases cortical excitability, and may modulate patterns of effective connectivity between functionally connected brain areas (e.g., Morishima et al. 2009).

To facilitate the identification of distant cortical regions engaged by stimulation of the left SPL, and those regions exhibiting the most task-related differences, the histograms depicted in Figure 5d represent the values of SCD and SCS for the *STM* (black) and *fixation* (white) conditions cumulated over the post-

TMS interval (0-400 ms) for all cortical areas. In each plot, areas are sorted from left to right by the area showing the highest SCD/SCS values in the *fixation* condition. As can be seen, induced currents were larger when TMS was applied during task performance in nearly all activated cortical areas, with particularly pronounced effects in bilateral BA 6 and BA 7. Lesser effects were also observed in several dorsal stream parietal and occipital areas that were not directly stimulated, including extrastriate areas BA 18 and BA 19, and inferior parietal areas BA 39 and BA 40.

This pattern of effective connectivity following stimulation of the SPL is generally consistent with cortico-cortical interactions mediated by the first subcomponent of the superior longitudinal fasciculus (SLF I). This fiber tract has been found to connect the medial and dorsal parietal cortex with dorsal BA 6, including the premotor and supplementary motor cortex, and prefrontal areas BA 9 and BA 46 (Schmahmann et al. 2007). Interestingly, the highest cumulative activation was not observed directly under the coil (BA 7), but in bilateral BA 6. Extracting the time course of the significant currents in each of these areas (Fig. 5e) reveals that currents were the strongest in BA 7 (red lines) approximately 5-10 ms after stimulation. This initial response was considerably stronger in the *STM* (solid) versus *fixation* (dashed) condition, tapering off fairly rapidly in each condition. By contrast, the initial evoked response in BA 6 (blue lines) occurs around 50 ms post-TMS (~40 ms after the maximal response in BA 7), and is of comparable magnitude in each condition. The observed response latency is consistent with previous cortical stimulation studies showing that it takes ~20-40 ms for TMS-evoked neural impulses to travel between connected cortical regions (see, e.g., Ilmoniemi et al.

1997; Massimini et al. 2005; Morishima et al. 2009). However, in contrast to BA 7, where TMS-evoked currents dissipated fairly quickly, the response in BA 6 remained elevated for several hundred milliseconds following stimulation. Additionally, although the initial TMS-evoked currents in BA 6 were of similar magnitude in the *STM* and *fixation* conditions, the prolonged oscillation evident in this area was substantially larger during task performance. The differential time course of activation in these areas explains the stronger focus on BA 6 evident in the spatial distribution plots depicted in Fig. 5c, and in the cumulative histograms shown in Fig. 5d.

Discussion

Previous research has revealed several exogenous factors contributing to observed variance in the electrical currents induced by TMS, which may account for variance in some of the effects of TMS on behavior. However, the endogenous neural factors contributing to these effects remain unclear. In the present study, we explored the influence of behavioral state on temporal and spectral properties of the TMS-ER. Our procedure was to deliver single pulses of TMS to the SPL both during the performance of a *STM* task and while subjects maintained central fixation, and to compare the resulting evoked response across conditions.

Results revealed increased amplitude and spatial spread of the TMS-ER during performance of the *STM* task relative to fixation. Specifically, when applied during the delay period of the spatial delayed-recognition task, TMS produced a larger evoked response from approximately 60-300 ms post-TMS. To more fully explore these effects, we computed several synthetic indices of cortical

responsiveness to TMS (Casali et al. 2010). These indices make it possible to characterize the effects of TMS on cortical activity and to quantitatively evaluate changes in the neural excitability and effective connectivity of different brain areas in different conditions. Results of this analysis revealed that task performance increased the overall strength of electrical currents induced by TMS, increased the spatial spread of TMS-evoked electrical activity to distal brain regions, and increased the ability of TMS to reset the phase of ongoing broadband cortical oscillations. Moreover, inspection of these results suggested that, in both behavioral conditions, the TMS-ER spread primarily to bilateral frontal and posterior regions connected to the SPL by known fiber tracts. However, the overall evoked response in each cortical area examined was larger when TMS was applied during task performance. These findings lay the groundwork for future work using this method to explore changes in patterns of effective connectivity during tasks requiring attention to or memory for different types of information.

In contrast to the behavioral state-related changes in the amplitude and spread of the TMS-ER, the natural frequency of the brain's response to TMS of the SPL did not change as a function of behavioral state – the estimated natural frequency was ~17 Hz in the *fixation* condition versus ~14Hz in the *STM* condition. Although these values were not significantly different from each other, they were somewhat lower than the natural frequency of 20 Hz observed following stimulation of the SPL (BA 7) in the study of Rosanova et al. (2009). Natural frequency estimates were more variable overall in the present study, and, in several cases, the spectral power of the TMS-ER averaged over the first 200 ms following stimulation revealed

two or more spectral peaks, including, most commonly, a pronounced low-frequency peak together with a high-frequency peak. A similar multi-frequency evoked response was observed by Thut et al. (2011) following the first pulse of a five pulse TMS train applied to the parietal cortex. The presence of this lower-frequency peak in the average global TMS-evoked spectral response likely contributed to the lower overall natural frequency values reported here.

Because TMS is known to evoke electrical activity at distant cortical sites (Ilmoniemi et al. 1997; Massimini et al. 2005), in addition to the targeted area (Paus et al. 2001), we also explored the effects of TMS on cortical areas that were not directly stimulated. As with the effective connectivity analysis, this analysis was conducted on source-localized data, which minimizes volume conduction effects, making it easier to observe the spread of electrical activity to distal cortical sites. In a previous study (Rosanova et al. 2009), direct stimulation with TMS produced alpha-band oscillations in the occipital cortex (BA19, $M = 11$ Hz), beta-band oscillations in the parietal cortex (BA7, $M = 20$ Hz), and high-beta/gamma-band oscillations in the frontal cortex (BA6, $M = 31$ Hz). Additionally, although the dominant frequency recorded globally at the scalp matched that of the stimulated area, each local cortical area tended to oscillate at a rate close to its own natural frequency even when not directly stimulated. Although only BA 7 was stimulated in the present study, the dominant frequency of oscillations observed at each local cortical area (BA 19, BA 7, and BA 6) were quite similar to the values reported by Rosanova and colleagues (2009), supporting the contention that the observed oscillations reflect local physiological mechanisms in each area. Interestingly,

however, in two cortical areas (BA 6 and BA 7) we also observed a second, lower-frequency oscillatory peak in the theta (BA 6, 7 Hz) and alpha (BA 7, 10 Hz) bands (as reflected in Figure 4). This pattern was particularly pronounced in the STM condition, raising the possibility that multiple oscillatory peaks in the parietal and frontal cortex may reflect synchronization of local cortical oscillations to parallel networks engaged in task performance (see also Thut et al. 2011).

Direct stimulation of the SPL also produced a pronounced low-frequency oscillation in the superior frontal cortex (BA 8), which was not examined in the study of Rosanova et al. (2009). This region of frontal cortex, including rostral BA 6, which contains the human homologue of the monkey FEF (Curtis and D'Esposito 2003), has been shown to be involved in the retention of spatial information in STM (e.g., Courtney et al. 1998; Curtis and D'Esposito 2003; Postle et al. 2000). Thus, this could reflect task-specific neural activity related to the performance of the STM task. An alternative possibility to this behavioral state-related effective connectivity account, however, is that the trial-to-trial unpredictability of the delivery of TMS in the STM condition may have produced a larger involuntary orienting response in this condition versus the fixation condition. In tests of STM in which a 3 sec-long train of 10 Hz repetitive TMS was delivered unpredictably during half of the delay periods of a block, for example, the TMS-ER to the first several pulses of the train induced a large-magnitude response at frontal midline electrodes that was not observed for the ensuing pulses of the train (Hamidi et al. 2009). Inspection of Fig. 5e argues against this alternative, however, in that it shows that the temporal profile

of the SCD at BA 6 and at BA 7 seems to share all the same components, although the time-varying changes in magnitude vary differently at the two regions.

Limitations of the present study

The present results suggest that performance of the STM task increased the excitability of the stimulated cortical area, as well as the spread of TMS-evoked currents to functionally connected areas; however, the TMS protocol used here only targeted a single cortical area with a fixed stimulation intensity. Conclusions regarding task-dependent changes in cortical excitability could be strengthened by varying the strength of stimulation and calculating the difference in stimulation intensity required to produce significant TMS-evoked currents. Additionally, it may be informative to stimulate cortical areas other than the SPL, such as task-relevant frontal areas (e.g., the FEF), which would allow exploration of task-dependent changes in the anterior-posterior spread of TMS-evoked oscillations. Stimulation of task-irrelevant areas may likewise support stronger conclusions regarding the functional relevance of the observed task-related differences.

Conclusions

The finding of reliable differences in several indices of the TMS-ER as a function of behavioral state (STM vs. fixation) is broadly consistent with previous findings that the TMS-ER differs in wakefulness vs. sleep (Massimini et al. 2005) and in wakefulness vs. anaesthetization (Ferrarelli et al. 2010). The manipulation of state is more subtle in the present study, however, and suggests that this approach may be promising for the study of task-related patterns of effective connectivity (see

also, Akaishi et al. 2010; Driver et al. 2009; Morishima et al. 2009), as well as for the study of neurological and psychiatric disease states.

Acknowledgments

We would like to thank David Sutterer and Michael Starrett for assistance with data collection, and Fabio Ferrarelli, Simone Sarasso, and Marcello Massimini for technical assistance.

Grants

This study was supported by grants MH88115-02 (J.S.J.), and MH064498-05 (B.R.P.) from the National Institute of Mental Health.

Disclosure/Conflict of Interest

The authors declare that the research described here was conducted in the absence of any commercial or financial relationships that could be construed as a potential conflict of interest.

Author Contributions

J.S.J. and B.R.P. designed research; J.S.J. performed research; J.S.J., B.K., and A.C. analyzed data; and J.S.J., B.K., and B.R.P. wrote the paper.

References

- Akaishi R, Morishima Y, Rajeswaren VP, Aoki S, and Sakai K.** Stimulation of the frontal eye field reveals persistent effective connectivity after controlled behavior. *The Journal of Neuroscience* 30: 4295-4305, 2010.
- Attneave F, and Arnoult MD.** Methodological considerations in the quantitative study of shape and pattern perception. *Psychological Bulletin* 53: 221-227, 1956.
- Berg P, and Scherg M.** A fast method for forward computation of multiple-shell spherical head models. *Electroencephalography and Clinical Neurophysiology* 90: 58-64, 1994.

- Bonato C, Miniussi C, and Rossini PM.** Transcranial magnetic stimulation and cortical evoked potentials: A TMS/EEG co-registration study. *Clinical Neurophysiology* 117: 1699-1707, 2006.
- Casali AG, Casarotto S, Rosanova M, Mariotti M, and Massimini M.** General indices to characterize the electrical response of the cerebral cortex to TMS. *NeuroImage* 49: 1459-1468, 2010.
- Casarotto S, Romero LR, Bellina V, Casali AG, Rosanova M, Pigorini A, Defendi S, Mariotti M, and Massimini M.** EEG responses to TMS are sensitive to changes in the perturbation parameters and repeatable over time. *PLoS ONE* 5: e10281, 2010.
- Courtney SM, Petit L, Maisog JM, Ungerleider LG, and Haxby JV.** An area specialized for spatial working memory in human frontal cortex. *Science* 279: 1347-1351, 1998.
- Curtis CE, and D'Esposito M.** Persistent activity in the prefrontal cortex during working memory. *Trends in Cognitive Sciences* 7: 415-423, 2003.
- Driver J, Blankenburg F, Bestmann S, Vanduffel W, and Ruff CC.** Concurrent brain-stimulation and neuroimaging for study of cognition. *Trends in Cognitive Science* 13: 319-327, 2009.
- Ferrarelli F, Massimini M, Sarasso S, Casali AG, Reidner BA, Angelini G, Tononi G, and Pearce RA.** Breakdown in cortical effective connectivity during midazolam-induced loss of consciousness. *Proceedings of the National Academy of Science USA* 107: 2681-2696, 2010.
- Friston KJ, Henson R, Phillips C, and Mattout J.** Bayesian estimation of evoked and induced responses. *Human Brain Mapping* 27: 722-735, 2006.
- Friston KJ, Penny W, Phillips C, Kiebel S, Hinton G, and Ashburner J.** Classical and Bayesian inference in neuroimaging: theory. *NeuroImage* 16: 465-483, 2002.
- Hamidi M, Slagter HA, Tononi G, and Postle BR.** Brain responses evoked by high-frequency repetitive TMS: An ERP study. *Brain Stimulation* 3: 2-14, 2009.
- Ilmoniemi R, Virtanen J, Ruohonen J, Karhu J, Aronen H, Naatanen R, and Katila T.** Neuronal responses to magnetic stimulation reveal cortical reactivity and connectivity. *Neuroreport* 8: 3537-3540, 1997.
- Jung TP, Makeig S, Humphreys C, Lee TW, McKeown MJ, Iragui V, and Sejnowski TJ.** Removing electroencephalographic artifacts by blind source separation. *Psychophysiology* 37: 163-178, 2000.
- Komssi S, Kahkonen S, and Ilmoniemi R.** The effect of stimulus intensity on brain responses evoked by transcranial magnetic stimulation. *Human Brain Mapping* 21: 154-164, 2004.
- Maldjian JA, Laurienti PJ, Kraft RA, and Burdette JH.** An automated method for neuroanatomic and cytoarchitectonic atlas-based interrogation of fMRI data sets. *NeuroImage* 19: 1233-1239, 2003.
- Maris E, and Oostenveld R.** Nonparametric statistical testing of EEG- and MEG-data. *Journal of Neuroscience Methods* 164: 177-190, 2007.
- Massimini M, Ferrarelli F, Huber R, Esser SK, Singh H, and Tononi G.** Breakdown of cortical effective connectivity during sleep. *Science* 309: 2228-2232, 2005.
- Mattout J, Phillips C, Penny WD, Rugg MD, and Friston KJ.** MEG source localization under multiple constraints: an extended Bayesian framework. *NeuroImage* 30: 753-767, 2006.

- Morishima Y, Akaishi R, Yamada Y, Okuda J, Toma K, and Sakai K.** Task-specific signal transmission from prefrontal cortex in visual selective attention. *Nature Neuroscience* 12: 85-91, 2009.
- Oostenveld R, Fries P, Maris E, and Schoffelen JM.** FieldTrip: Open source software for advanced analysis of MEG, EEG, and invasive electrophysiological data. *Computational Intelligence and Neuroscience* 2011: 2011.
- Paus T, Sipila P, and Strafella A.** Synchronization of neuronal activity in the human sensori-motor cortex by transcranial magnetic stimulation: a combined TMS/EEG study. *Journal of Neurophysiology* 86: 1983-1990, 2001.
- Perrin F, Pernier J, Bertrand O, and Echallier JF.** Spherical splines for scalp potential and current density mapping. *Electroencephalography and Clinical Neurophysiology* 72: 184-187, 1989.
- Phillips C, Mattout J, Rugg MD, Maquet P, and Friston KJ.** An empirical Bayesian solution to the source reconstruction problem in EEG. *NeuroImage* 24: 997-1011, 2005.
- Postle BR, Berger JS, Taich AM, and D'Esposito M.** Activity in human frontal cortex associated with spatial working memory and saccadic behavior. *Journal of Cognitive Neuroscience* 12, suppl. 2: 2-14, 2000.
- Rosanova M, Casali A, Bellina V, Resta F, Mariotti M, and Massimini M.** Natural frequencies of human corticothalamic circuits. *Journal of Neuroscience* 29: 7679-7685, 2009.
- Schmahmann JD, Pandya DN, Wang R, Dai G, D'Arceuil HE, de Crespigny AJ, and Wedeen VJ.** Association fibre pathways of the brain: parallel observations from diffusion spectrum imaging and autoradiography. *Brain* 130: 630-653, 2007.
- Thut G, Veniero D, Romei V, Miniussi C, Schyns P, and Gross J.** Rhythmic TMS causes local entrainment of natural oscillatory signatures. *Current Biology* 21: 1176-1185, 2011.
- Tikhonov AN, and Arsenin VY.** *Solutions of ill-posed problems*. Winston, Washington: 1977.
- Virtanen J, Ruohonen J, Naatanen R, and Ilmoniemi R.** Instrumentation for the measurement of electrical brain responses to transcranial magnetic stimulation. *Medical and biological engineering and computing* 37: 322-326, 1999.
- Walsh V, and Pascual-Leone A.** *Transcranial Magnetic Stimulation: A Neurochronometrics of Mind*. Cambridge: MIT Press, 2003.

Figure Captions

Figure 1. Behavioral task, timing of TMS stimulation, and targeted brain area. Subjects performed a delayed-recognition task requiring memory for the locations of four sequentially-presented shapes across a 3.75 s delay interval. On half of trials, two TMS pulses were applied at an average frequency of .5 Hz during the delay. In a separate trial block (not shown), TMS pulses were applied at an average rate of .5 Hz while subjects maintained fixation on a centrally-presented cue (as in the delay period of the STM task). In each case, TMS was applied to a portion of the left superior parietal lobule (SPL) anterior and medial to the intraparietal sulcus (IPS).

Figure 2. ERP waveforms and topographical plots of the TMS-evoked response (TMS-ER) across behavioral conditions. Grand-averaged ERPs of the TMS-ER recorded over a cluster of peripheral (**a**) and central (**b**) electrodes (see inset topographical plots in each panel) in the *STM* (red) and *fixation* (blue) conditions. (**c**) Results of cluster analysis revealing a larger amplitude low-frequency TMS-ER in the *STM* versus *fixation* condition beginning ~60 ms and extending to ~300 ms post-TMS. Black squares highlight electrodes where negative clusters (*fixation* > *STM*) were observed, and black stars highlight positive clusters (*STM* > *fixation*).

Figure 3. Time-frequency plots showing the spectral transform of the TMS-ER recorded globally at the scalp for each behavioral condition. The TMS-evoked spectral responses were similar in the *STM* (**a**) and *fixation* (**b**) conditions, with prominent responses in the beta and theta frequency bands (dashed horizontal lines in each panel). The natural frequency, calculated separately for each subject as the frequency exhibiting maximal power from 20-200 ms post-TMS, did not differ significantly across conditions. The red dashed box in each plot indicates time points and frequencies where significant clusters were observed.

Figure 4. Time-frequency representations of the source localized data showing the TMS-evoked spectral response across behavioral conditions for four cortical areas of interest. For each area examined, TMS to the SPL elicited similar patterns of spectral power when applied during the delay-period of the *STM* task (**a**) and during central fixation (**b**). Panel (**c**) shows the average TMS-evoked power from 20-200 ms post-TMS in the *STM* (red) and *fixation* (blue) conditions for each area.

Figure 5. Computation of synthetic measures of cortical responsiveness to TMS across behavioral conditions. Average ($n=16$) global estimates (**a**) and time-course (**b**) of significant current density (SCD), significant current scattering (SCS), and broad-band phase-locking (bPL) over the whole brain and the full post-stimulus period in the *STM* (solid) and *fixation* (dashed) conditions. Panel (**c**) shows the spatial distribution of SCD, SCS, and bPL in the *STM* (left) and *fixation* (right) conditions averaged across subjects and plotted in MNI space. Panel (**d**) shows cumulative SCD and SCS in each cortical area sorted by the area showing maximal SCD/SCS values in the *fixation* condition. Panel (**e**) shows the time course of significant TMS-evoked currents in BA 7 versus BA 6 for each behavioral condition averaged across subjects. Error bars in panel (**a**) reflect the standard error of the mean.

Figure 1.

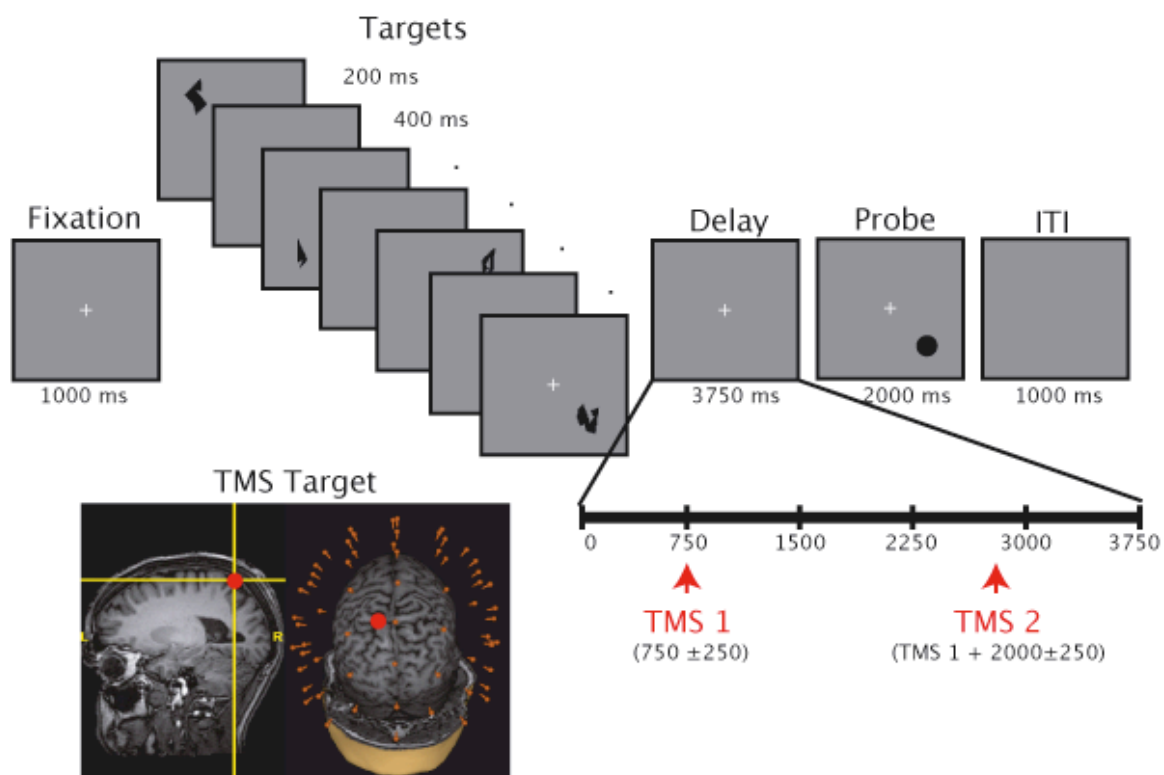


Figure 2.

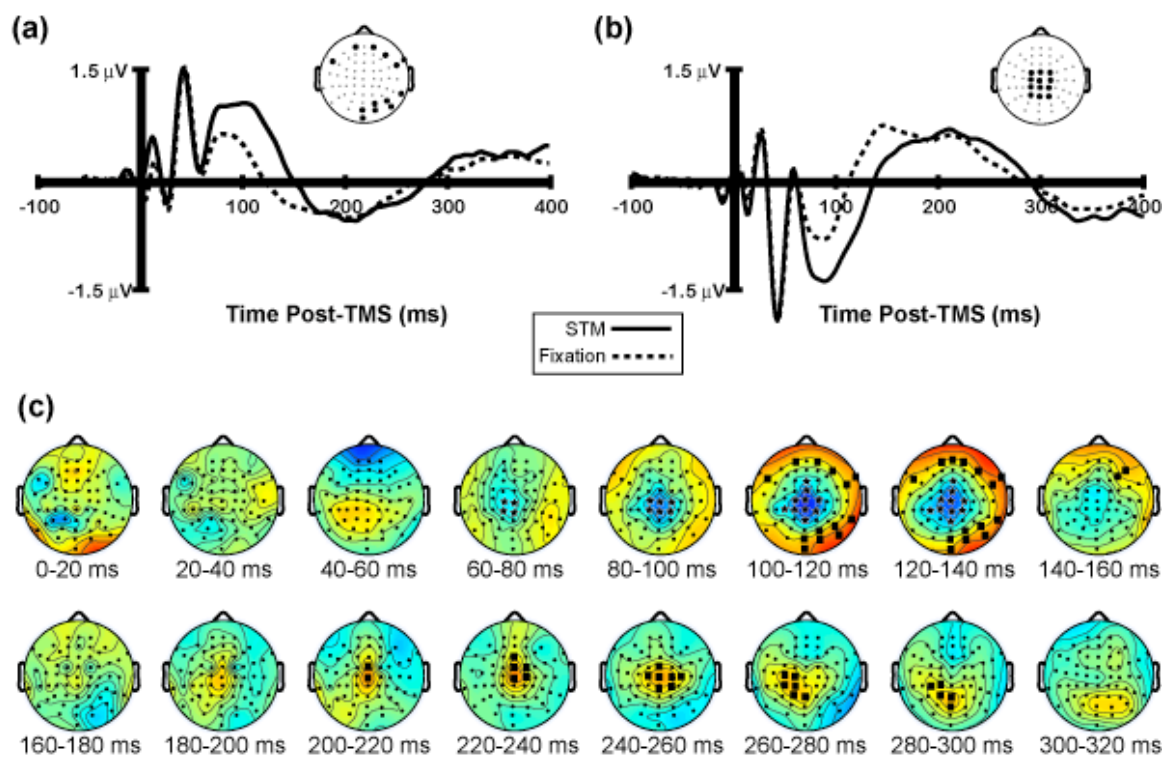


Figure 3.

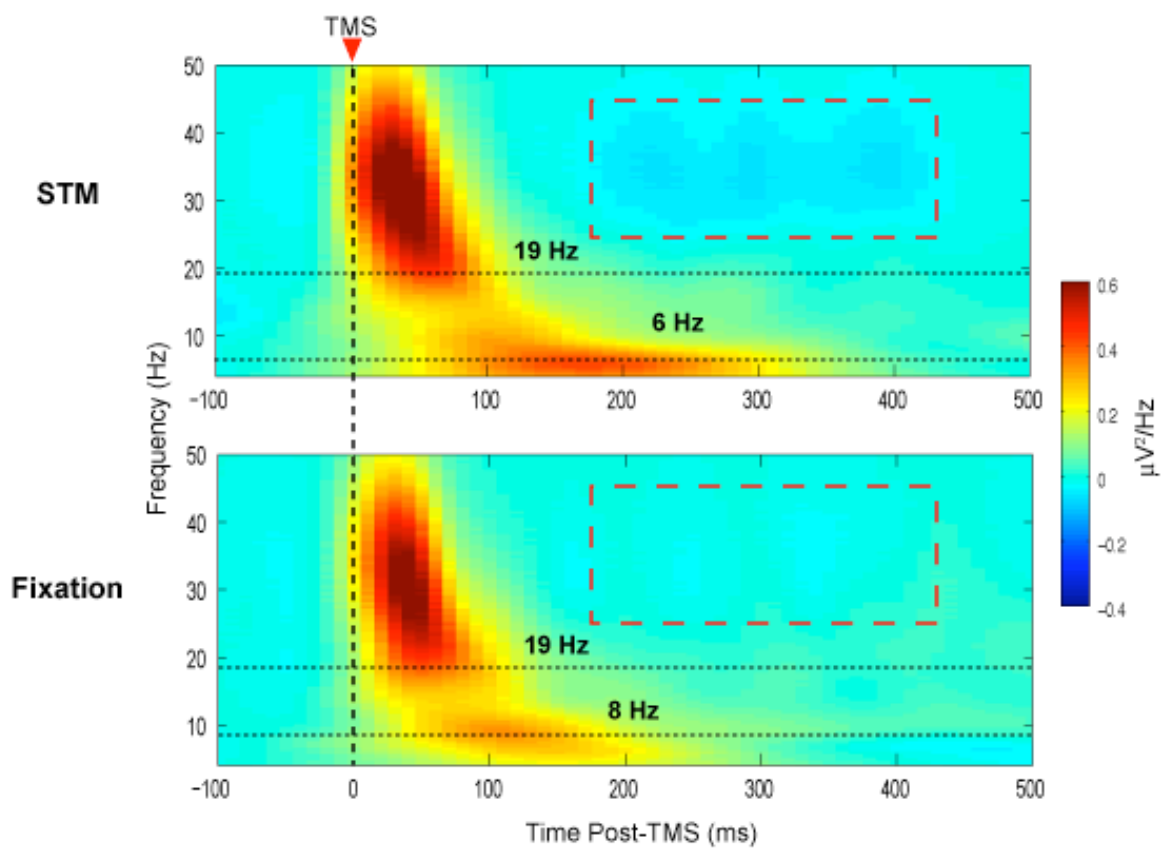


Figure 4.

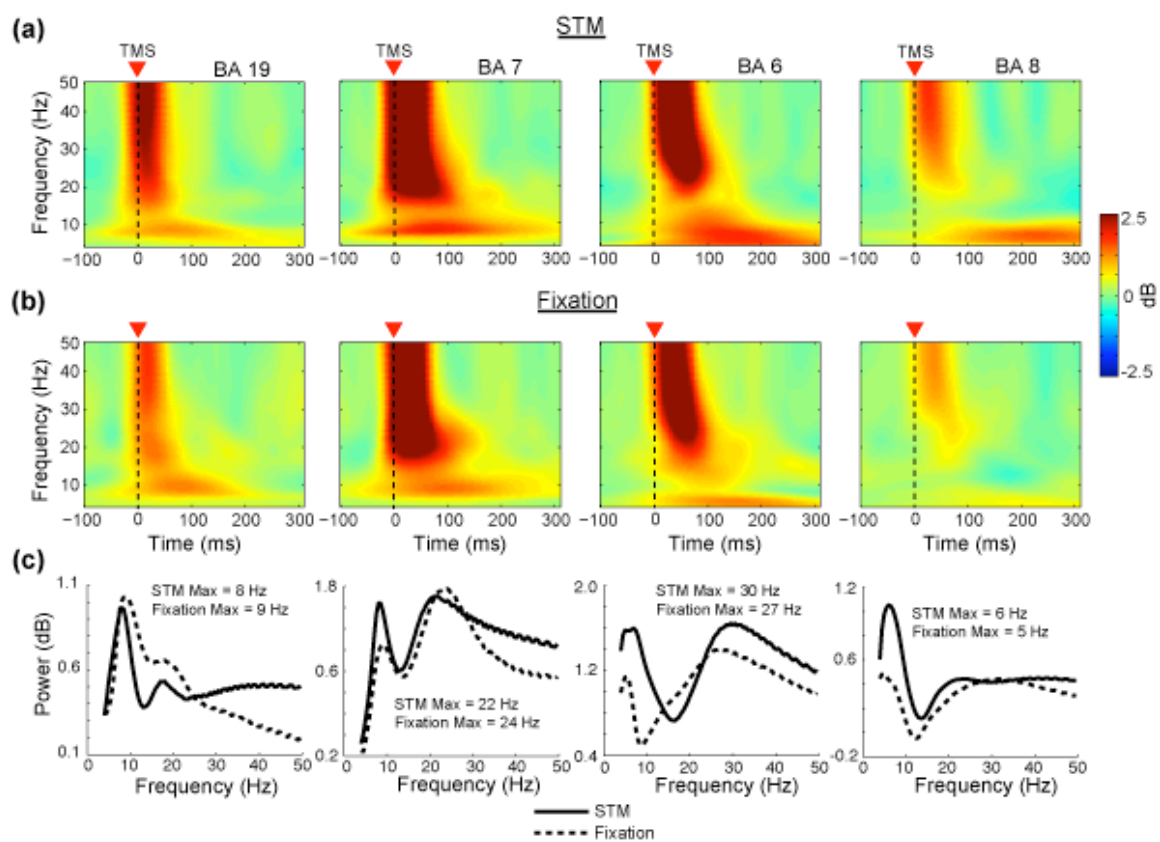


Figure 5.

